Characterization of time-resolved fluorescence response measurements for distributed optical-fiber sensing

Elena Sinchenko,[1] W. E. Keith Gibbs,[1] Claire E. Davis,[2] and Paul R. Stoddart[1,*]

[1]Faculty of Engineering and Industrial Science, Swinburne University of Technology, VIC 3122, Australia

[2]Air Vehicles Division, Defence Science and Technology Organisation, 506 Lorimer Street, Fishermans Bend, VIC 3207, Australia

*Corresponding author: pstoddart@swin.edu.au

A distributed optical-fiber sensing system based on pulsed excitation and time-gated photon counting has been used to locate a fluorescent region along the fiber. The complex Alq_3 and the infrared dye IR-125 were examined with 405 and 780 nm excitation, respectively. A model to characterize the response of the distributed fluorescence sensor to a Gaussian input pulse was developed and tested. Analysis of the Alq_3 fluorescent response confirmed the validity of the model and enabled the fluorescence lifetime to be determined. The intrinsic lifetime obtained (18.2 ± 0.9 ns) is in good agreement with published data. The decay rate was found to be proportional to concentration, which is indicative of collisional deactivation. The model allows the spatial resolution of a distributed sensing system to be improved for fluorophores with lifetimes that are longer than the resolution of the sensing system.   © 2010 Optical Society of America

OCIS codes: 120.4825, 060.2370, 300.6280.

1. Introduction

A common approach to long-range distributed measurement in optical fibers is based on optical time-domain reflectometry, which utilizes the characteristics of backscattering against time when a short pulse of light is launched into the waveguide. Distributed optical-fiber sensing systems with evanescent field excitation of a fluorescent region surrounding the fiber core are of interest for monitoring broad-area chemical distributions. It has been shown that distributed chemical sensors can be achieved by immobilizing suitable reagents into the cladding of plastic-clad silica (PCS) optical fiber [1–5].

Despite the number of potentially important applications, relatively few practical distributed chemical sensing systems based on evanescent field interactions have been reported [6–10]. This is primarily due to the difficulty of protecting the optical-fiber sensor while allowing sufficiently sensitive interaction between the target chemical species and the guided light in the fiber core. Ongoing improvements in cladding formulations have allowed progress to be made in this regard for absorption-mediated sensors [2], but fluorescence-based systems appear to have been neglected due to issues with sensitivity, stability, and fluorescence lifetime effects. Nevertheless, fluorescence-based techniques potentially provide a powerful transduction mechanism for chemical events, with a large number of fluorescent indicators available to detect a wide range of chemical species.

Because of the low excitation and coupling efficiency via the evanescent field interaction, an approach based on photon counting has been employed to increase the sensitivity of the detection system. This is analogous to distributed temperature sensors that use photon counting to detect weak anti-Stokes

Raman scattering. Previous work has shown that this approach can be extremely effective when combined with appropriate background correction procedures [11].

For an effective distributed sensor, the physical and chemical properties of the target species and the particular parameters of the detection system should be taken into account as they jointly dictate the sensitivity, selectivity, and accuracy of the eventual measurement. The prime characterizing parameters may be defined as spatial resolution, fiber path length, sensitivity, noise level, and system dynamic range. The interaction between the lifetime of the fluorophore, the type and length of the fiber system, and the shape of the excitation pulse are critical to interpret the response of the sensor.

This paper describes a model that has been developed to characterize this interaction and predict the behavior of the fluorescent response at the detector. Experimental results are presented that validate the model for two different fluorophores with substantially different lifetimes in a laboratory-scale quasi-distributed arrangement. The fluorescence from the aluminum complex Alq_3, excited at 405 nm, and from the dye IR-125, excited at 780 nm, was measured at the input end of the fiber by a time-gated detection system. The Alq_3 system has potential application for the detection of corrosion in aluminum alloys.

This model provides a significant improvement in spatial resolution for fluorophores with lifetimes that are longer than the resolution of the sensing system.

2. Experiment

The multimode optical fiber used for the sensing system had a 200 μm diameter pure silica core with a proprietary plastic cladding and a nylon buffer layer (APC200/300N Fiberguide Industries). The buffer layer was removed using a surgical blade and the cladding was dissolved by soaking in chromic–sulphuric acid for 30 min. The cladding residue was subsequently removed with a lint-free tissue. Care was taken during the handling process to ensure minimal disturbance to the core surface. This was checked by measuring the fiber transmission at 780 nm when the declad fiber section was immersed in a series of dimethyl sulfoxide (DMSO) and water solutions of different refractive index. The transmission was observed to decrease smoothly as the refractive index approached that of the core (1.45) with no discontinuities that would indicate scattering or loss from inhomogeneities on the core surface. In addition, a microscopic examination of the core surface was conducted to inspect for damage and no damage was observed for the fibers tested.

The experimental arrangement is shown in Fig. 1. An optical-fiber section of 0.2 m length was declad as described above and immersed in solutions of either the complex Alq_3 for 405 nm excitation, or the infrared dye IR-125 for 780 nm excitation. The declad section was approximately 3 m from the end of an 80 m
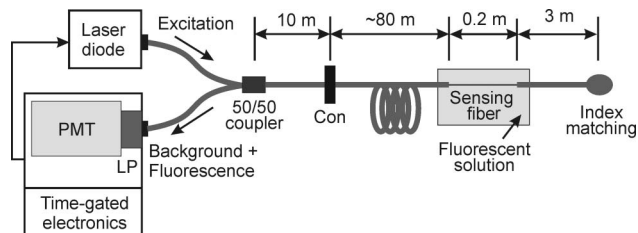

Fig. 1. Experimental arrangement: LP, long-pass filter; Con, temporary connector.

length of fiber. The extended fiber length was designed to attenuate cladding modes near the excitation source and, thus, provide stable propagation conditions in the declad section. The 405 nm laser diode excitation source (OptoTech Ltd, Australia) had pulse widths of between 3 and 5 ns (FWHM) with an approximately Gaussian shape and a repetition frequency of 25 kHz. The 780 nm laser source was developed in house using a Sanyo DL7140-201S laser diode and a PCO-7110 laser diode driver module to provide Gaussian pulses of approximately 4 ns FWHM at the same repetition rate and coupled into an optical fiber. A 50/50 coupler that separated the forward and backward propagating light was custom made for the large core fiber (Diamond SA, Switzerland).

The detection system employed long-pass filters (LP) to remove the respective excitation wavelengths, and the photomultiplier tube (PMT, Hamamatsu R928) was operated in the photon-counting mode. The Alq_3 complex and the IR-125 dye fluoresce in the 450–600 nm and 800–900 nm regions, respectively. The PMT quantum efficiency varies from 14% at 500 nm to 0.5% at 850 nm. Photon counts were accumulated by the time-gated electronics in bins of 2 ns width, which corresponds to a length resolution along the fiber of 0.2 m, assuming a propagation velocity of 2×10^8 m/s. An accumulation time of 10 min was used to obtain adequate signal-to-noise discrimination. The resultant bin accumulations can be regarded as waveforms of the fluorescence that originate at a distance along the fiber corresponding to the return time of flight as designated by the bin number. As the propagation time through the length of the declad sensor section in the present experiment is of the order of the time resolution, the fluorescence can be regarded as originating from a point source.

The Alq_3 complex was prepared by the reaction of aluminum nitrate with 8-hydroquinone (8-HQ) in ethanol solvent. This reaction has been proposed as a method of detecting aluminum corrosion via the presence of Al^{3+} ions [12]. The IR-125 dye was dissolved in a 50/50 mix of DMSO/water solvent chosen to obtain a refractive index close to that of the original cladding (1.42).

Complementary continuous-wave measurements of forward-propagating fluorescence and laser excitation were performed with either a spectrum analyzer or the LP/PMT combination at the output end of the fiber. These measurements agreed with the

published fluorescence spectra [13–15] and showed that the fluorescence intensity was proportional to the absorbed excitation power in each case.

A typical detected signal is shown in Fig. 2. This represents the time-domain response of the detection system when the declad fiber section was immersed in a 5×10^{-3} M solution of Alq_3. Reflection peaks from the coupler, connector, and the distal end of the fiber can be clearly identified. The prototype nature of the coupler and connector for this fiber type results in relatively high reflection signals. These could be reduced by employing telecommunication-grade couplers and fusion-splicing techniques.

3. Results

A. Model and Curve Fitting

The time-dependence of the fluorescence can be obtained from the solution of the rate equation for a two-level system excited with a Gaussian shaped pulse. Thus,

$$\dot{n} - \frac{n}{\tau} = kNI_0 \exp\left(-\frac{1}{2}\left(\frac{t-T}{\sigma}\right)^2\right), \quad (1)$$

where n, N give the respective populations of the fluorescing level and the ground state of the two-level system, k represents the absorption, and I_0 is the exciting pulse amplitude. The Gaussian excitation is centered at time T with width parameter σ and τ is the lifetime of the fluorescing level.

Equation (1) has the solution, for $n \ll N$,

$$n(t) = k\sigma NI_0 \sqrt{\frac{\pi}{2}} \exp\left(\frac{2\sigma^2}{\tau^2}\right) \exp\left(-\frac{t-T}{\sigma}\right)$$
$$\times \left[1 + \mathrm{erf}\left(\frac{1}{\sqrt{2}}\left(\frac{t-T}{\sigma} - \frac{\sigma}{\tau}\right)\right)\right].$$

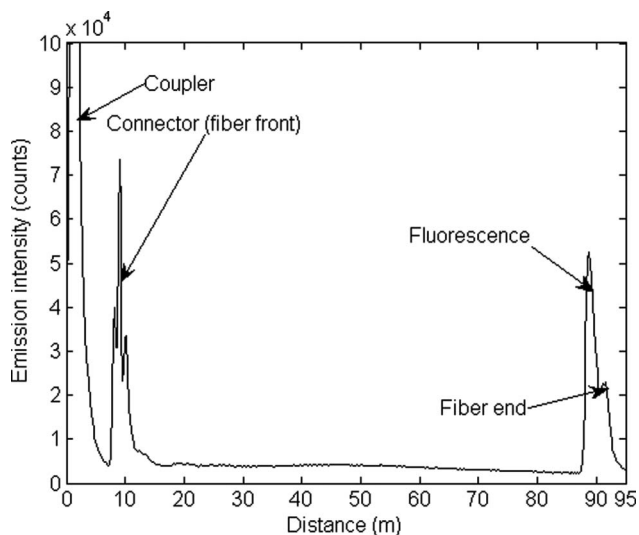The fluorescence intensity is proportional to the n and can be written

Fig. 2. Time-resolved response of the distributed sensor, plotted in terms of distance traveled in the optical fiber.
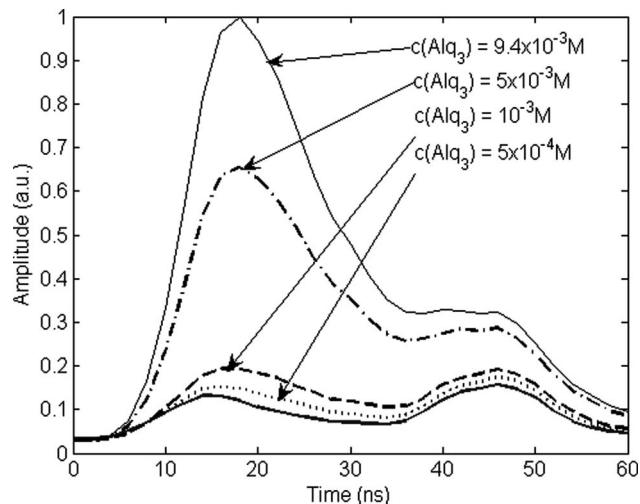

Fig. 3. Alq_3 fluorescence waveforms for range of concentrations. The solid curve represents background signal from the ethanol solvent. The waveform for the concentration of 0.1×10^{-3} M has been excluded for the sake of clarity.

$$I_t(t) = K \exp\left(-\frac{t-T}{\sigma}\right)\left[1 + \mathrm{erf}\left(\frac{1}{\sqrt{2}}\left(\frac{t-T}{\sigma} - \frac{\sigma}{\tau}\right)\right)\right], \quad (2)$$

where K is the collection of the time-independent terms and erf is the error function.

B. Alq_3 Fluorescence

The fluorescence waveforms for a range of Alq_3 concentrations are shown in Fig. 3. The optical time delay due to the 80 m length of fiber preceding the sensor has been removed for clarity. Also shown is the background signal (solid line) from the ethanol solvent. The background signal arises from backscattered excitation from the sensor section that leaks through the LP filter. The secondary peak that
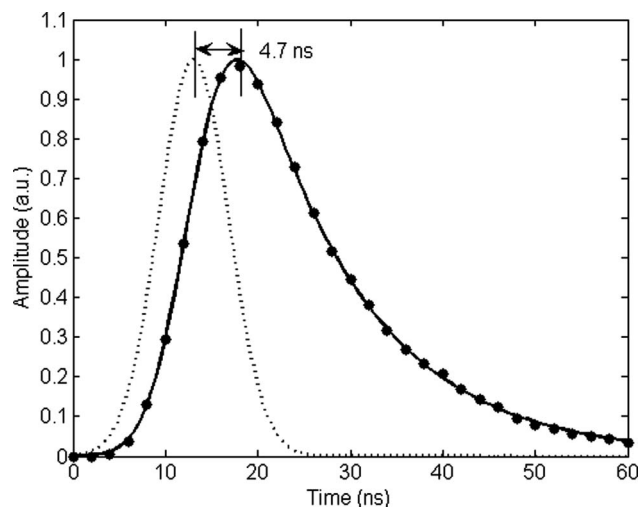

Fig. 4. Alq_3 fluorescence (9.4×10^{-3} M, circles) after subtraction of the background component due to the ethanol solvent. The model fit [Eq. (2), solid curve] is shown together with a reconstruction of the excitation pulse from the fitted parameters (dashed curve).

occurs approximately 30 ns after the signal from the declad section coincides with reflection from the end of the fiber. Subtraction of the background signal results in single-peaked waveforms, a typical example of which is shown in Fig. 4. The conspicuous trailing edge of these waveforms is indicative of a significant fluorescence lifetime, in contrast with the IR-125 results discussed later.

Also included in Fig. 4 is the model fit using Eq. (2); the fitted parameters σ, τ, and ΔT, which represents a time delay between maximums of excitation and fluorescence pulses, are given in Table 1 for the concentrations shown. It is apparent from the consistency of the fitted σ that the model developed provides a good description of the situation. The fitted values of σ correspond to a FWHM of 9 ns, which is somewhat larger than those expected from the FWHM of the excitation pulse (3–5 ns). This broadening of the measured waveform can be attributed to the effect of the finite bin width (2 ns) and jitter in the synchronization between the excitation pulse and the bin gates during the 10 min counting accumulation time.

Also shown in Fig. 4 is a reconstruction of the Gaussian excitation pulse using the values of σ and ΔT in Table 1 for the concentration of 9.4×10^{-3} M. This shows that the peak of the fluorescence waveform is delayed as expected. The distance along the fiber from which the fluorescence originates can be calculated more precisely by correcting for the time delay between the excitation and fluorescence response. For the data shown in Fig. 4, for example, the delay is 4.7 ns, which is equivalent to 0.47 m in terms of range.

The decrease in τ with concentration is indicative of collisional de-excitation of the fluorescence level of the Alq$_3$, as can be seen in Fig. 5 where the decay rate is shown to be linearly dependent on the concentration. The larger errors at low concentrations are a consequence of the lower fluorescence signal. The errors are reduced as the signal increases at higher concentrations or for longer acquisition times. The intrinsic lifetime of 18.2 ± 0.9 ns at zero concentration is comparable with the previously observed value of 10.22–22.7 ns in different organic solvents [16].

The peak fluorescence signal is shown to be proportional to concentration in Fig. 6; from this, it is estimated that the minimum concentration that can be

Table 1. Fitted Model Parameters for Alq$_3$ Fluorescence Waveforms for the Concentrations Shown Together with the Delay of the Fluorescence Peak From the Peak of the Reconstructed Gaussian Input[a]

Alq$_3$ Concentration (M)	σ (ns)	τ (ns)	ΔT (ns)
9.4×10^{-3}	3.73 ± 0.04	12.3 ± 0.1	4.70 ± 0.03
5.0×10^{-3}	3.82 ± 0.05	14.0 ± 0.1	5.02 ± 0.23
1.0×10^{-3}	4.11 ± 0.20	17.6 ± 0.6	5.71 ± 0.17
0.5×10^{-3}	4.10 ± 0.30	17.7 ± 1.7	5.71 ± 0.16
0.1×10^{-3}	4.19 ± 0.26	17.9 ± 2.4	5.82 ± 0.23

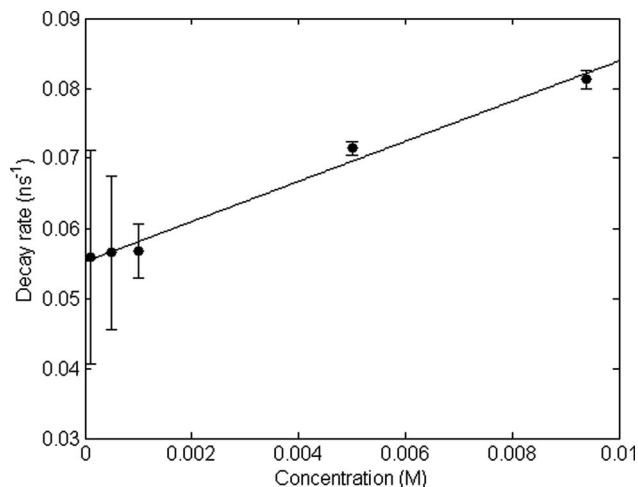[a]The standard errors of the fitted parameters are also shown.

Fig. 5. Concentration dependence of the Alq$_3$ fluorescence decay rate. The zero concentration intercept corresponds to an intrinsic lifetime of 18.2 ± 0.9 ns.

detected is $\sim 5 \times 10^{-5}$ M or ~ 20 ppm (wt.) over an exposed length of 0.2 m. Greater or lesser sensitivities would be expected for greater or lesser lengths of exposed fiber. The sensitivity could also be improved by increasing the laser repetition rate and/or the total accumulation time.

C. IR-125 Fluorescence

In contrast with Alq$_3$, the lifetime of fluorescence from IR-125 is known [17] to be much smaller than 1 ns, which is shorter than the measurement resolution of this system; hence, the fluorescence waveform would not be expected to show a significant trailing edge. A typical waveform is shown in Fig. 7, where it can be seen that the waveform is roughly symmetrical with little evidence of a significant fluorescent lifetime, τ. However, model fitting using Eq. (2) gives a time delay of approximately 2.2 ns and τ of 3.7 ns (8.6 ns in terms of FWHM). Those parameters could
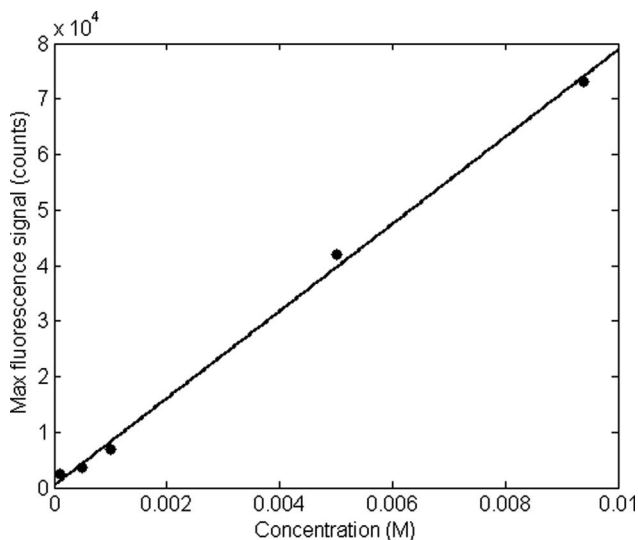

Fig. 6. Dependence of peak Alq$_3$ fluorescence on concentration (circles) together with a linear fit.
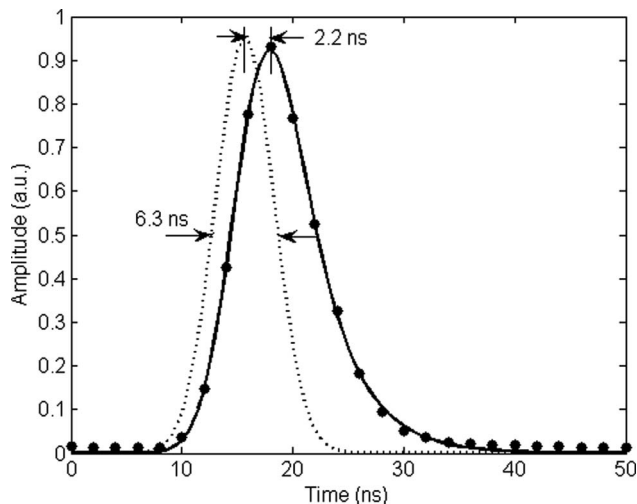
Fig. 7. Fluorescence waveform for the IR-125 dye at a concentration 5×10^{-5} M (circles) together with the model fit [Eq. (2)].

be associated with an instrument response function. The FWHM of 8.6 ns is in reasonable accordance with the resolution of 6 ns obtained for distributed temperature sensing with a similar detection system [11].

It is interesting to note that the background noise level for IR-125 is much lower than that observed in the wavelength range relevant to the Alq_3. This may be due to the fact that the low-OH silica optical fiber used in this study is not optimized for use at wavelengths in the UV–violet range. The reduced quantum efficiency of the R928 PMT in the near-infrared wavelength range does not appear to play a significant role in this regard. In any event, the background level is sufficiently reduced to allow a detection sensitivity of 2×10^{-6} M ($\sim$1.2 ppm) for IR-125. This result suggests that evanescent field excitation of fluorescence can provide a sufficiently sensitive detection mechanism for distributed chemical sensing, under appropriate conditions.

4. Conclusion

The use of declad silica-core optical fiber for the detection of fluorescence from the region surrounding the exposed core has been demonstrated in a pulsed time-gated system that has the potential of localizing the source of fluorescence along the fiber length. The system was used to examine two different fluorescent environments: the complex Alq_3 excited at 405 nm and the infrared dye IR-125, excited at 780 nm. The former environment is potentially relevant to the early detection of aluminum cations produced as a byproduct during the early stages of corrosion.

Although the experiments were conducted on a laboratory-scale quasi-distributed arrangement, the results would be applicable to a fully distributed system, where the complete fiber length was clad with sensitive material. The results show that the spatial resolution of the detection system can be limited by the lifetime of the fluorophore. Analysis of the fluorescence waveforms confirmed the use of a model

incorporating Gaussian excitation in the signal processing procedure could significantly improve the spatial resolution. The model also allows the fluorescence lifetime to be determined, with the results obtained showing good agreement with published data. It is estimated that the minimum concentration of Alq_3 that can be detected under these experimental conditions is $\sim$5 × 10^{-5} M or $\sim$20 ppm (wt.) over an exposed length of 0.2 m. The detection limit for IR-125 was found to be 2×10^{-6} M ($\sim$1.2 ppm). Given the relatively small number of molecules that fall within the range of the evanescent field and contribute to the fluorescent signal, these results suggest that the evanescent field excitation mechanism can provide sensitive detection of chemical distributions. Greater or lesser sensitivities would be expected for greater or lesser lengths of exposed fiber.

References

1. S. R. Cordero, H. Mukamal, A. Low, E. P. Locke, and R. A. Lieberman, "A fiber optic sensor for nerve agent," Proc. SPIE **6378**, 63780U (2006).
2. S. R. Cordero, H. Mukamal, A. Low, M. Beshay, D. Ruiz, and R. A. Lieberman, "Fiber optic sensor coatings with enhanced sensitivity and longevity," Proc. SPIE **6377**, 63770C (2006).
3. R. A. Potyrailo, A. W. Szumlas, T. L. Danielson, M. Johnson, and G. M. Hieftje, "A dual-parameter optical sensor fabricated by gradient axial doping of an optical fibre," Meas. Sci. Technol. **16**, 235–241 (2005).
4. R. A. Potyrailo and G. M. Hieftje, "Use of the original silicone cladding of an optical fiber as a reagent-immobilization medium for intrinsic chemical sensors," Fresenius' J. Anal. Chem. **364**, 32–40 (1999).
5. R. A. Potyrailo and G. M. Hieftje, "Optical time-of-flight chemical detection: absorption-modulated fluorescence for spatially resolved analyte mapping in a bidirectional distributed fiber-optic sensor," Anal. Chem. **70**, 3407–3412 (1998).
6. R. A. Lieberman, L. L. Blyler, and L. G. Cohen, "A distributed fiber optic sensor based on cladding fluorescence," J. Lightwave Technol. **8**, 212–220 (1990).
7. R. A. Potyrailo and G. M. Hieftje, "Optical time-of-flight chemical detection: spatially resolved analyte mapping with extended-length continuous chemically modified optical fibers," Anal. Chem. **70**, 1453–1461 (1998).
8. P. E. Henning, A. Benko, A. W. Schwabacher, P. Geissinger, and R. J. Olsson, "Apparatus and methods for optical time-of-flight discrimination in combinatorial library analysis," Rev. Sci. Instrum. **76**, 062220 (2005).
9. H. Mukamal, S. R. Cordero, D. Ruiz, M. Beshay, and R. A. Lieberman, "Distributed fiber optic chemical sensor for hydrogen sulfide and chlorine detection," Proc. SPIE **6004**, 600406 (2005).
10. S. R. Cordero, M. Beshay, A. Low, H. Mukamal, D. Ruiz, and R. A. Lieberman, "A distributed fiber optic chemical sensor for hydrogen cyanide detection," Proc. SPIE **5993**, 599302 (2005).
11. P. R. Stoddart, P. J. Cadusch, J. B. Pearce, D. Vukovic, C. R. Nagarajah, and D. J. Booth, "Fibre optic distributed temperature sensor with an integrated background correction function," Meas. Sci. Technol. **16**, 1299–1304 (2005).
12. G. McAdam, P. J. Newman, I. McKenzie, C. Davis, and B. R. W. Hinton, "Fiber optic sensors for detection of corrosion within aircraft," Struct. Health Monit. **4**, 47–56 (2005).

13. R. Philip, A. Penzkofer, W. Bäumler, R. M. Szeimies, and C. Abels, "Absorption and fluorescence spectroscopic investigation of indocyanine green," J. Photochem. Photobiol. A **96**, 137–148 (1996).

14. S. A. Soper and Q. L. Mattingly, "Steady-state and picosecond laser fluorescence studies of nonradiative pathways in tricarbocyanine dyes—implications to the design of near-IR fluorochromes with high fluorescence efficiencies," J. Am. Chem. Soc. **116**, 3744–3752 (1994).

15. T. Hoshi, K. Kumagai, K. Inoue, S. Enomoto, Y. Nobe, and M. Kobayashi, "Electronic absorption and emission spectra of Alq(3) in solution with special attention to a delayed fluorescence," J. Lumin. **128**, 1353–1358 (2008).

16. V. V. N. R. Kishore, K. L. Narasimhan, and N. Periasamy, "On the radiative lifetime, quantum yield and fluorescence decay of Alq in thin films," Phys. Chem. Chem. Phys. **5**, 1386–1391 (2003).

17. H. Lee, M. Y. Berezin, M. Henary, L. Strekowski, and S. Achilefu, "Fluorescence lifetime properties of near-infrared cyanine dyes in relation to their structures," J. Photochem. Photobiol. A **200**, 438–444 (2008).